

Predicting the Navigation Performance of Underwater Vehicles

Brian Bingham

Abstract—In this paper we present a general framework for predicting the positioning uncertainty of underwater vehicles. We apply this framework to common examples from marine robotics: standalone long baseline (LBL) positioning and integrated LBL reference and Doppler velocity log (DVL) dead-reckoning.

The approach is based on formulating positioning as an estimation problem. Using simple sensor models for the most common information sources, we show how the Cramér Rao lower bound can be used to predict the system-level navigation performance. The resulting three dimensional covariance matrix is then summarized using scalar performance metrics based on the notion of dilution of precision (DOP), a well-known concept from the global positioning system (GPS) community. To illustrate this general tool, we present the answers to a few particular questions:

- How does the baseline length affect the solution for standalone LBL positioning?
- When using DVL and heading odometry, how precise is the combined DVL/LBL solution?
- For an integrated DVL/LBL solution, what is the required update rate from the absolute reference to constrain odometry drift?
- What is the relative importance of heading, odometry and range precision for overall performance?

We substantiate our estimation framework through experimental evidence which shows that the analytical predictions are consistent with performance in the field.

I. INTRODUCTION

The challenge of underwater positioning—determining the location of submerged assets—continues to limit our capability to explore, understand and operate in the marine environment. Robotic technologies such as remotely operated vehicles (ROVs), autonomous underwater vehicles (AUVs) and gliders have pushed back the frontier of scientific, military and industrial programs (some examples include [1]–[5]). This expansion of robotic work in the deep ocean has been accompanied by constant innovation in underwater navigation. Some innovations are specific to the marine environment. For example, long baseline (LBL) range-based positioning and Doppler velocity log (DVL) dead-reckoning were both created specifically for ocean applications. Other advances have transferred new tools from terrestrial navigation to the challenge of positioning submerged assets. Examples include inertial measurement units (IMUs) and fiber-optic gyro (FOG) instruments. Finally, there has been considerable work focused on combining these disparate information sources into a navigation estimate, the most common examples address the integration of LBL and DVL

instruments [6]. The last 30 years of research and operations have left the vehicle designer with a variety of options for instrumentation hardware, operational configurations and integration algorithms. We present an analytical framework to aid in the design of these increasingly complex systems.

The goal of this paper is to answer some important questions for practical robotic underwater navigation. Because operational solutions typically include range measurements providing an absolute reference, we focus on quantifying how range measurements are included in modern, multi-modal navigation solutions. It is our hope that this article will contribute a tool for making design decisions, providing researchers, engineers and operators with methods for quantifying the trade-offs when including range observations into estimates of location.

II. CLOSELY RELATED WORK

The foundations of this work are well established. There is a large body of literature on stochastic sensor models, estimation prediction using the Cramér Rao lower bound (CRLB) and metrics for summarizing uncertainty. The main contributions of this work is the creation of a sensor model to capture the salient dynamics of conventional underwater navigation and the experimental evaluation of the resulting performance predictions. Additionally, the results of this analysis provide practical guidance for designers of marine robotic systems.

Previous researchers have proposed stochastic models for underwater localization. Deffenbaugh applied the CRLB to standalone acoustic positioning [7]. More recently, Eustice presented a combined navigation model to support maximum likelihood estimation based on one-way acoustic travel times [8]. The sensor model presented here builds on the standalone solution by incorporating odometry information. By considering exclusively the along-track and across-track directions, we generate generalizable conclusions on the relationship between the various characteristics of the complete navigation solution.

III. APPROACH

Navigation is an estimation problem. Predicting the performance of the estimator requires three things: a stochastic model, a method of relating measurement uncertainty to estimate uncertainty and performance metrics to summarize the estimate quality. In this work we apply simple models—abstractions which relate noisy observations to the underlying quantities we wish to estimate. For navigation we estimate position based on noisy measurements that might

B. Bingham is an Assistant Professor of Mechanical Engineering, University of Hawaii at Manoa, 2450 Dole St., Holmes Hall 302, Honolulu, HI. bsb@hawaii.edu

include range distances to fixed locations, velocity over the bottom, heading and a variety of other information sources.

Part of our approach is based on Gaussian distribution noise models. These models are not proposed as full quantifications of the complex uncertainty, but instead as useful tools that provide pertinent predictions for making design trade-offs. This is an important distinction. Our goal is not to fully characterize the noise measurements, but instead to predict the performance of these systems in such a way as to aid their operation and design. The experimental portion of this work is designed to substantiate the applicability of these simple models.

To quantify how the measurement uncertainty leads to estimate uncertainty we use the Cramér Rao lower bound [9]. This technique provides a prediction of position uncertainty, typically a three-dimensional covariance matrix. The CRLB is a measure of how much information about the vehicle position is available in our measurements of range, velocity and heading.

A. Models for Navigation Uncertainty

The first component of our estimation framework is a set of observation models for spherical positioning, velocity observations and heading observations.

1) *Spherical Positioning Measurement Model*: Spherical positioning is based on observing individual range values (z_{r_i}) between known fixed beacon locations (\mathbf{x}_{b_i}) and an unknown mobile host position (\mathbf{x}_h) where the individual range measurements is indexed by i .

$$z_{r_i} = \|\mathbf{x}_h - \mathbf{x}_{b_i}\| + w_{r_i} \quad (1)$$

We consider the additive noise in each measurement (w_{r_i}) as an independent, zero-mean, Gaussian variable with variance σ_r^2 .

$$w_{r_i} \sim \mathcal{N}(0, \sigma_r) \quad (2)$$

The utility of this Gaussian error model along with the measurement of the σ_r statistic will be discussed in the experimental results that follow.

2) *Odometry Measurement Model*: A DVL has become a standard instrument for underwater robotics because of the quality of the solution and ease of use. Dead-reckoning with a DVL consists of fusing the measured velocity over the seafloor with an accurate heading reference to estimate distance traveled. The DVL instrument provides independent measurements of velocity (v_k) in each of three dimensions (indexed by k). Transforming these sensor frame measurements into a local coordinate frame requires knowledge about sensor and vehicle attitude. Heading is the most important measurement for this coordinate rotation [10]. Again we use a simple additive Gaussian noise model to represent the heading (ψ) measurement.

While it is possible to carry forward the complete three dimensional uncertainty formulation [11], for the clarity we present the two-dimensional case. This is a non-limiting simplification for two reasons: most underwater vehicles are passively stable in pitch and roll, furthermore pitch and roll

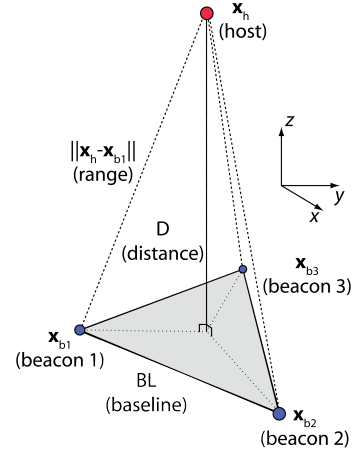


Fig. 1. This figure illustrates the 3D positioning trilateration problem. The three fixed acoustic nodes are arranged in an equilateral triangle (\mathbf{x}_{b_i}) for $i = \{1, 2, 3\}$ and the mobile host (\mathbf{x}_h) a distance (D) above the plane containing the three fixed nodes. The extent of the fixed nodes is captured with the baseline parameter (BL).

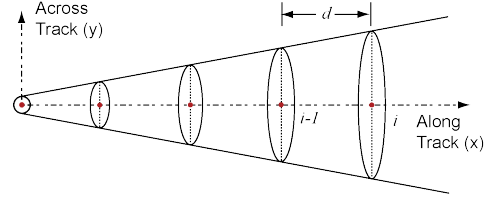


Fig. 2. Illustration of odometry uncertainty dynamics. The ellipses illustrate the $1\text{-}\sigma$ uncertainty in the along track (x) and across track (y) directions. Five discrete vehicle positions are shown, indexed by i . The distance between consecutive positions is d .

are typically measured much more accurately than heading. We also consider the uncertainty along track to be independent of the uncertainty across track. This consideration captures the dominant dynamics of error growth and allow us to simplify our two-dimensional model, preserving intuition. This approach leads to an observation model of odometry where each discrete measurement of incremental distance (z_{o_j} , where j is the index for velocity measurements).

$$z_{o_j} = (\mathbf{x}_{h_j} - \mathbf{x}_{h_{j-1}}) + \mathbf{w}_o \quad (3)$$

The additive noise is characterized by a two-dimensional covariance matrix (Σ_o) in the along track and across track directions.

$$\mathbf{w}_o \sim \mathcal{N}(0, \Sigma_o) \quad (4)$$

$$\Sigma_{o_i} = \begin{bmatrix} t\sigma_v^2 & 0 \\ 0 & d^2\sigma_\psi^2 \end{bmatrix} \quad (5)$$

The diagonal matrix in Equation (5) is a consequence of the independent along track and across track uncertainty growth.

Figure 2 is an illustration of this simple odometry model. The aspect ratio of error ellipses increases with time, illustrating the linear growth of the along track uncertainty (growing with distance traveled) and the growth of the along track position with the square root of time.

B. Predicting Performance Using The Cramér Rao Lower Bound

As an estimation problem we consider the estimation of an unknown parameter vector \mathbf{x} based on a set of observations \mathbf{z} with known probability density $p_z(z; x)$. When it exists, the CRLB gives the lower bound on the variance of *any* valid unbiased estimator $\hat{\mathbf{x}}()$ for \mathbf{x} [9].

1) *The Cramér Rao Lower Bound for Spherical Positioning*: We apply this tool to the spherical positioning problem by linearizing the measurement model [7]. The individual range measurements of Equation (1) are assembled into a measurement vector of length n .

$$\mathbf{Z}_r = \{z_{r_i}\}_0^{n-1} \quad (6)$$

$$= \mathbf{h}(\mathbf{x}_h, \mathbf{x}_b) + \mathbf{w}_r \quad (7)$$

where $\mathbf{h}()$ is the non-linear function for spherical positioning and \mathbf{w}_r is a zero mean random vector with covariance Σ_r .

$$\mathbf{w}_r \sim \mathcal{N}(0, \Sigma_r) \quad (8)$$

The CRLB can be calculated by linearizing the measurement model about an operating point \mathbf{x}_{h_o} , i.e., let $\mathbf{x}_h = \mathbf{x}_{h_o} + \delta\mathbf{x}_h$.

$$\mathbf{Z}_r \approx \mathbf{h}(\mathbf{x}_{h_o}, \mathbf{x}_b) + \mathbf{C}(\mathbf{x}_{h_o}, \mathbf{x}_b)\delta\mathbf{x}_h + \mathbf{w}_r \quad (9)$$

The Jacobian ($\mathbf{C}(\mathbf{x}_{h_o}, \mathbf{x}_b)$) is evaluated at a particular vehicle position \mathbf{x}_{h_o} and for each fixed transponder location \mathbf{x}_b . For this linearized, Gaussian noise measurement model the CRLB is a matrix combination of the the Jacobian, representing the current system geometry, and the measurement covariance.

$$\Lambda = \left[\mathbf{C}(\mathbf{x}_{h_o}, \mathbf{x}_b)^T \Sigma_r^{-1} \mathbf{C}(\mathbf{x}_{h_o}, \mathbf{x}_b) \right]^{-1} \quad (10)$$

The CRLB is the best-case estimate of the state covariance of the positioning solution based on (1) the geometry of the static acoustic beacons, (2) the location of the host relative to the beacons and (3) the range uncertainty.

2) *The Cramér Rao Lower Bound for Integrated Positioning*: To apply this tool we must express the complete observation model for integrated absolute and relative positioning measurements. We present this in two dimensions, recalling that x is the along track dimension and y is the across track dimension. The result is a combined measurement model including n measurements of the absolute x and y positions along with $n - 1$ measurements of the relative distance traveled in each direction.

$$\mathbf{Z}_c = [\mathbf{A}] \begin{Bmatrix} x_1 \\ \vdots \\ x_n \\ y_1 \\ \vdots \\ y_n \end{Bmatrix} + \Sigma_c \quad (11)$$

where

$$[\mathbf{A}] = \begin{bmatrix} \mathbf{I}_{n \times n} & \mathbf{0}_{n \times n} \\ \mathbf{0}_{n \times n} & \mathbf{I}_{n \times n} \\ \Delta_{n-1 \times n} & \mathbf{0}_{n-1 \times n} \\ \mathbf{0}_{n-1 \times n} & \Delta_{n-1 \times n} \end{bmatrix} \quad (12)$$

$$\Delta_{n-1 \times n} = \begin{bmatrix} 0 \\ \vdots \\ \mathbf{I}_{n-1} \\ 0 \end{bmatrix} - \begin{bmatrix} \mathbf{I}_{n-1} & \vdots \\ & 0 \end{bmatrix} \quad (13)$$

$$\Sigma_c = \begin{bmatrix} \sigma_p^2 \mathbf{I}_{2n} & \mathbf{0} & \mathbf{0} \\ \mathbf{0} & \sigma_v^2 (dt) \mathbf{I}_{n-1} & \mathbf{0} \\ \mathbf{0} & \mathbf{0} & \sigma_\psi^2 (dx)^2 \mathbf{I}_{n-1} \end{bmatrix} \quad (14)$$

where \mathbf{I}_n is an $n \times n$ identity matrix, dt is the elapsed time between absolute position updates and dx is the corresponding distance traveled along track between successive absolute position updates.

C. Metrics for Navigation Uncertainty

Using the CRLB and the preceding measurement models we can predict the positioning performance in the form of the full covariance matrix (Σ_{x_h}).

$$\Sigma_{x_h} = \begin{bmatrix} \sigma_x^2 & \sigma_{xy}^2 & \sigma_{xz}^2 \\ \sigma_{xy}^2 & \sigma_y^2 & \sigma_{yz}^2 \\ \sigma_{xz}^2 & \sigma_{yz}^2 & \sigma_z^2 \end{bmatrix} \quad (15)$$

We use scalar metrics adapted from the GPS community [12] to succinctly summarize the performance: the horizontal dilution of position (HDOP— σ_{HDOP}) and the 50% circular error probable (CEP).

$$\sigma_{HDOP} = \frac{\sqrt{\sigma_x^2 + \sigma_y^2}}{\sigma_r} \quad (16)$$

$$\text{CEP} \approx 0.59 (\sigma_L + \sigma_S) \quad (17)$$

where σ_L and σ_S are the major and minor axes of the uncertainty ellipse, the eigenvalues of the two-dimensional covariance matrix¹.

In order to provide consistent comparisons between modes of positioning, we introduce two non-standard metrics: *horizontal precision* (HP) and *normalized circular error probable* (NCEP).

$$\text{HP} = \sqrt{\sigma_x^2 + \sigma_y^2} \quad (18)$$

$$\text{NCEP} \approx \frac{0.59 (\sigma_L + \sigma_S)}{\sigma_r} \quad (19)$$

IV. ANALYTICAL PREDICTIONS

A. Standalone LBL Solution

Figure 1 illustrates the specific geometry considered in the following analysis. By varying a single non-dimensional parameter, the ratio of the distance to the baseline length

¹The linear approximation of the CEP can be derived from the estimate covariance. The difference between the true CEP and the approximation of Equation (17) is less than 1.5% when the uncertainty ellipse has a low aspect ratio ($0.5\sigma_L \leq \sigma_S \leq \sigma_L$), otherwise a quadratic approximation can be substituted [13].

(D/BL), and using the CRLB to predict the positioning performance, we quantify how the baseline length affects host positioning quality. The distance parameter (D) is the length of line extending perpendicular from a plane containing the fixed beacons to the mobile host.

To determine the CRLB lower bound (Equation (10)) we evaluate the Jacobian ($C(\mathbf{x}_{h_o}, \mathbf{x}_b)$) from Equation (9) for the spherical positioning observations. Using the specific geometry illustrated in Figure 1,

Since we have assumed the range measurements are independent and identically distributed, the covariance of the observations (Σ_r) is simply a diagonal matrix where each element on the diagonal is the variance in the range observations (σ_r). This leads to a simple expression for the CRLB.

$$\Lambda = \sigma_r^2 \begin{bmatrix} 2 \left(\frac{r}{BL}\right)^2 & 0 & 0 \\ 0 & 2 \left(\frac{r}{BL}\right)^2 & 0 \\ 0 & 0 & \frac{1}{3} \left(\frac{r}{D}\right)^2 \end{bmatrix} \quad (20)$$

We evaluate the performance metrics HDOP and NCEP (Equation (16) and Equation (19) respectively) by using the approximation $\left(\frac{r}{BL}\right) \approx \left(\frac{D}{BL}\right)$. This approximation has small error for even modest values of D/BL^2 .

$$\text{HDOP} \approx 2 \left(\frac{D}{BL}\right) \quad (21)$$

$$(22)$$

Equation (21) is the analytical predictions for the relationship between the relative baseline size and the positioning performance of a range based system. This simple linear relationship is a “rule of thumb” to inform operational trade-offs.

B. Integrated LBL/DVL Solution

Using the CRLB framework we predict the navigation performance for integrated solutions that employ both absolute and relative positioning techniques. Figure 3 illustrates this prediction for a large range of system parameters. To calculate the HDOP we normalize the uncertainty in the x and y directions with the overall absolute positioning uncertainty (σ_p). To evaluate the HDOP for a particular integrated navigation solution requires quantifying the following parameters:

- Position uncertainty (σ_p) which is the standard deviation of the overall absolute position reference.
- Along track uncertainty (σ_{along}) which is a function of the velocity uncertainty (σ_v) and the acoustic update rate (dt).
- Across track uncertainty (σ_{across}) which is a function of the heading uncertainty (σ_ϕ) and the distance traveled between acoustic updates (dx).

To interpret the results in Figure 3 we can examine the three regions labeled A, B and C. On the left, in region A, the along track uncertainty is much smaller than the absolute

²The error is less than 10% for $D \geq 0.68(BL)$ and the error is less than 1% for $D \geq 2.3(BL)$.

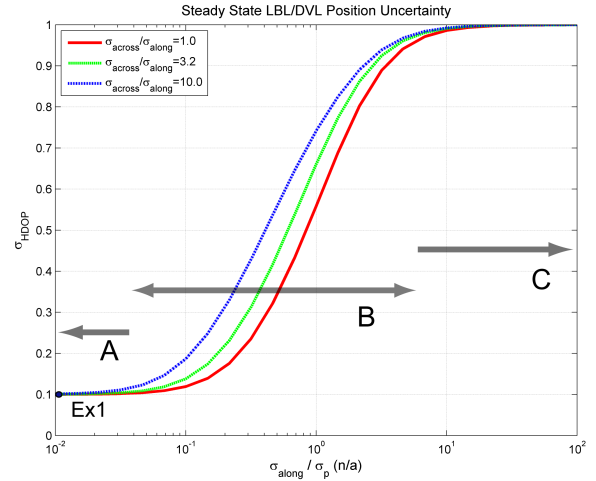


Fig. 3. This figure quantifies the trade-offs in designing an integrated positioning solution using absolute (LBL) and relative (DVL/Heading) positioning. The vertical axis shows predictions of the overall HDOP. The point labeled “Ex1” and corresponds to the illustrative example described below.

position uncertainty, i.e., the velocity error is small and that the update rate is relatively fast, preventing large drift in the relative positioning between updates. The result, indicated by a low HDOP, is that the overall positioning uncertainty is 10% of the standalone absolute positioning. Because of the accuracy of the relative measurements between individual absolute updates, the information from each absolute reference cycle accumulates, lowering the overall uncertainty. In fact, this asymptote achieves the lower bound for the overall uncertainty of $1/\sqrt{n}$, where n is the number of absolute position updates. In this case $n = 100$.

Another interesting aspect of this limiting case is that the across track uncertainty does not affect the resulting performance. This is an important result because for solutions that employ only relative positioning (dead-reckoning), the heading reference is a key determinate of performance. In contrast, the prediction illustrated in Figure 3 shows that when both absolute and relative positioning are combined and the velocity measurements have low uncertainty, the quality of the heading reference has little impact on the overall performance.

Region C, in the far right of Figure 3, illustrates the performance prediction for the opposite extreme when the relative positioning is poor compared to the absolute reference. In this case the HDOP asymptotically approaches 1.0, indicating that the standalone absolute position uncertainty is equivalent to the combined uncertainty.

To further the illustration we present an example based on a typical operational configuration for underwater vehicles: a 1,200 kHz RDI DVL ($\sigma_v = 3$ mm/s), an Octans true north heading reference ($\sigma_\psi = 0.1$ degrees) and Benthos LBL transponders ($\sigma_r \approx 3.0$ m). We assume a representative velocity of 1.0 m/s for the purposes of demonstration. These sensor parameters would place this system in Region A of Figure 3 (labeled “Ex1” in the figure) where the odometry

significantly improves the standalone acoustic positioning performance. Based on the predicted uncertainty, the required acoustic positioning update rate would be $t < 68$ s, i.e., the LBL position updates would need to arrive roughly each minute to take full advantage of the synergies between LBL, DVL and heading information.

V. EXPERIMENTAL RESULTS

The preceding analytical predictions are predicated on the applicability of simple models and additive, Gaussian noise. In particular, we claim that the techniques of the GPS community can be applied to underwater range-based positioning. Here we describe a range-only positioning experiment designed to test this hypothesis.

A. Positioning System Overview

The Sonic High Accuracy Ranging and Positioning System (SHARPS) is a general purpose high-frequency, spread spectrum navigation tool capable of precise time-of-flight range measurement. This system has been used to provide an accurate position reference in a variety of operating scenarios including deep-sea archaeology surveys [1], [14], operational support for the Jason-Medea two-body ROV system [15] and tank installations to support academic research [16].

B. Setup and Procedure

To directly observe the effect of baseline length on positioning performance we measured the mobile host location at a sequence of locations. At each location we made an average of 320 range measurements to each of the fixed beacons (see Figure 4). A coarse median filter was used to reject outliers caused by the dense multipath structure of the shallow pool environment. We used the range measurements to solve 3D spherical positioning problem using a real-time non-linear least-squares estimator³ and to calculate the non-normalized CEP and HP performance metrics for a set of stations between 0.83 and 11.43 m from the fixed beacons. To calculate the normalized NCEP and HDOP metrics required an estimate of the range uncertainty. The z component of the position covariance provides an estimate of the range uncertainty, i.e., $E[\hat{\sigma}_z] = 0.42\text{cm} \approx \sigma_r$. This procedure was intended to reproduce the scenario illustrated in Figure 1.

VI. DISCUSSION

Figure 5 illustrates the comparison between the analytical predictions of Section IV-A and the experimental results of Section V. There are two similar analytical predictions in Figure 5. The ‘‘Theory’’ prediction is for the idealized geometry in Figure 1, and the ‘‘Simulation’’ prediction results from numerically evaluating the CRLB for the actual geometry used in the test.

A linear fit of the empirical evidence for the HDOP metric shows strong correlation: R^2 of 0.93. This leads to the most important conclusion of this comparison: both the analytical

³It can be shown that the least-squares method is an efficient estimator for the non-linear spherical positioning problem, i.e., the least-squares algorithm achieves the CRLB.

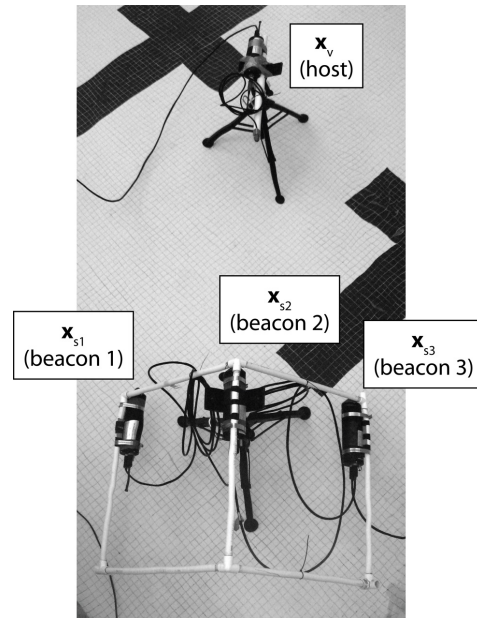


Fig. 4. Annotated photo of experimental setup. The three beacons in the lower part of the image are fixed to a frame where the baseline between 1 and 2 and between 2 and 3 are both 0.59 m. The host is located at a variable distance away from the beacon network. Shown here the host is approximately .2 m from the beacons.

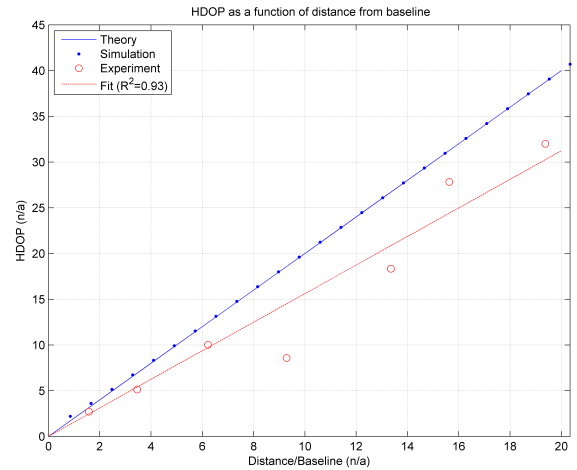


Fig. 5. This figure illustrates the HDOP as a function of the normalized distance between the mobile host and the fixed acoustic network. Four scenarios are shown for comparison: (1-Theory) theoretically predicted closed form solution for equilateral triangle with baseline, (2-Simulation) simulation results for right triangle, (3-Experiment) experimental results from SHARPS pool testing with a right triangle with 0.59 m baseline, (4-Fit) linear regression best-fit results.

prediction and experimental evidence show a consistent linear relationship between positioning performance and the (D/BL) ratio, just as predicted by the analytical framework proposed earlier.

While both the analytical and experimental results have a linear form, the linear coefficients are significantly different. The fractional difference in coefficients is 18% for the NCEP metric and 24% for the HDOP metric. We believe that this

is most likely a consequence of variance in our estimate of range uncertainty used to normalize the HDOP and NCEP metrics. The mean range variance of 0.42 cm had a standard deviation of 0.13 cm, 32% of the mean. This suggests that the actual range uncertainty could be lower which would account for the discrepancy.

VII. CONCLUSIONS

The preceding sections present an analytical framework for predicting the performance of navigation solutions for underwater vehicles. This framework uses the Cramér Rao lower bound to combine models of navigation observations to produce succinct scalar metrics of positioning performance. The experimental evidence substantiates the validity of these simple models. In particular we derive analytically, and then show empirically, that the uncertainty in the range-only positioning solution degrades linearly with the relative size of the fixed baseline. We also extend this analysis to illustrate the interplay between accuracy and precision necessary for understanding the trade-offs in designing an integrated navigation solution.

To introduce this approach we presented specific questions of importance for marine operations. Using this framework we have illustrated the following answers to those questions:

- All else being equal, the precision of the positioning solution is linearly related to the effective baseline length (see Equation (21)).
- The overall precision of an integrated DVL/LBL positioning solution is a function of the performance of each component and the LBL update rate. If designed correctly, the overall performance of this integrated solution provides a much more precise solution than either standalone solution. The actual performance can be predicted using Figure 3.
- For the DVL/LBL configuration typical of oceanographic operations, an absolute position fix should be acquired roughly each minute to take full advantage of the complementary nature of the two information sources.
- The relative impact of heading, odometry and range precision on the overall navigation system performance can be inferred through general results similar to Figure 3.

While the particular results are important, the generalizable conclusions have more impact. This information-based framework is a general purpose tool for predicting the performance of potential sensor and algorithm combinations. As a design tool, the ability to predict performance allows vehicle designers to make quantitative trade-offs when it comes to combining and configuring the variety of commercially available navigation solutions.

A. Future Work

The experimental work described here substantiates the applicability of Gaussian noise and linearized sensor models for range-only positioning. A similar experiment could be done to validate the random walk models used to incorporate the dead-reckoning contribution to positioning uncertainty.

VIII. ACKNOWLEDGMENTS

We wish to thank Marine Sonic Ltd., Thom Wilcox and Professor David Mindell (MIT) for supporting the experimental equipment. Also, Andrea Striz was particularly helpful in executing the experiments.

We also wish to thank the reviews who provided detailed comments that greatly improved this manuscript. An extended version of this article is available at: <http://www2.hawaii.edu/~bsb/>.

REFERENCES

- [1] D. R. Yoerger and D. A. Mindell, "Precise navigation and control of an ROV at 2200 meters depth," in *Proceedings of ROV '92*, San Diego, CA, June 1992.
- [2] H. Singh, A. Can, R. Eustice, S. Lerner, N. McPhee, O. Pizarro, and C. Roman, "Seabed AUV offers new platform for high-resolution imaging," *EOS, Transactions of the AGU*, vol. 85, no. 31, pp. 289,294–295, August 2004.
- [3] K. Vestgard, N. Storkersen, and J. Sortland, "Seabed surveying with Hugin AUV," in *Proceedings of the 11th International Symposium on Unmanned Untethered Submersible Technology*, Durham, NH, August 1999.
- [4] B. Allen, R. Stokey, T. Austin, N. Forrester, R. Goldsborough, M. Purcell, and C. von Alt, "REMUS: A small, low cost AUV; system description, field trials and performance results," in *Proceedings of the MTS/IEEE Oceans Conference*, vol. 2. Halifax, NS: MTS/IEEE, October 1997, pp. 994–1000.
- [5] U. S. Navy, "The Navy unmanned undersea vehicle (UUV) master planning," Department of the Navy, Tech. Rep., November 2004. [Online]. Available: <http://www.chinfo.navy.mil/navpalib/technology/uuvmppdf>
- [6] L. L. Whitcomb, D. R. Yoerger, and H. Singh, "Combined Doppler/LBL based navigation of underwater vehicles," in *Proceedings of the International Symposium on Unmanned Untethered Submersible Technology*, Durham, NH, August 1999.
- [7] M. Deffenbaugh, J. G. Bellingham, and H. Schmidt, "The relationship between spherical and hyperbolic positioning," in *Proceedings of the MTS/IEEE Oceans Conference*, Ft. Lauderdale, Florida, 1996.
- [8] R. Eustice, L. Whitcomb, H. Singh, and M. Grund, "Experimental results in synchronous-clock one-way-travel-time acoustic navigation for autonomous underwater vehicles," *Robotics and Automation, 2007 IEEE International Conference on*, pp. 4257–4264, April 2007.
- [9] Y. Bar-Shalom, X.-R. Li, and T. Kirubarajan, *Estimation with Applications to Tracking and Navigation*. John Wiley and Sons, Inc, 2001.
- [10] J. C. Kinsey and L. L. Whitcomb, "In situ alignment calibration of attitude and doppler sensors for precision underwater vehicle navigation: Theory and experiment," *IEEE Journal of Oceanic Engineering*, vol. 32, no. 2, pp. 286–299, Apr. 2007.
- [11] R. Eustice, L. Whitcomb, H. Singh, and M. Grund, "Recent advances in synchronous-clock one-way-travel-time acoustic navigation," in *Proceedings of the MTS/IEEE Oceans Conference*, Sept. 2006, pp. 1–6.
- [12] D. Kaplan, *Understanding GPS*. Artech House Publisher, 1996.
- [13] W. Nelson, "Use of circular error probability in target detection," MITRE Corporation, United States Air Force Hanscom Air Force Base, Tech. Rep. ESD-TR-88-109, May 1988.
- [14] J. Delgado, Ed., *Encyclopedia of Underwater and Maritime Archaeology*. Yale University Press, 1997.
- [15] B. Bingham, D. Mindell, T. Wilcox, and A. Bowen, "Integrating precision relative positioning into JASON/MEDEA ROV operations," *Marine Technology Society (MTS) Journal*, vol. 40, no. 1, pp. 87–96, Spring 2006.
- [16] J. C. Kinsey, D. A. Smallwood, and L. L. Whitcomb, "A new hydrodynamics test facility for UUV dynamics and control research," in *Proceedings of the MTS/IEEE Oceans Conference*, San Diego, CA, September 2003.